P13

Acamprosate intestinal absorption is partly paracellular and partly carrier mediated

Franek F[1], Neuhoff S[2], Rasmussen KF[1] and Steffansen B[1]

[1]Faculty of Health and Medical Sciences, University of Copenhagen, Universitetsparken 2, Copenhagen, Denmark
[2]Simcyp Ltd (a Certara Company), Blades Enterprise Centre, John St, Sheffield, S2 4SU, UK.

frans.franek@sund.ku.dk

Introduction

Acamprosate is a taurine analogue administered in oral dosage at 666 mg three times a day to treat alcohol dependence. It's a small MW (181.2 g/mole), hydrophilic (LogP = -3.57) sulfonic acid (pKa = 1.8) drug substance. The molecular structure of acamprosate is shown in Figure 1.

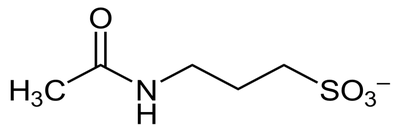

Figure 1. *Molecular structure of acamprosate*

Acamprosate is a BCS Class III drug substance, *i.e.* a high solubility, low permeability drug with an oral bioavailability of 11%. Furthermore, negligible acamprosate metabolism is observed and it is primarily excreted by the kidneys. Thus, acamprosate is unique with respect to intestinal permeability is limiting its absorption after oral administration. However, the relative roles of paracellular permeability (P_{para}) passive diffusion-driven transcellular permeability (P_{trans}) and transcellular carrier-mediated permeability (P_{car}) in intestinal absorption of acamprosate, is controversial[1-3].

Aim

The aim of this study is to investigate the rate-determining intestinal absorption of acamprosate in man by PBPK-modelling and simulation

Methods

Mechanistic Passive Permeability (MPP) Model

A MPP-model was developed in MATLAB (Release 2012b, The Math Works, Natick, United States) and was applied to estimate acamprosate effective intestinal passive permeability in human ($P_{eff,\ passive}$).

$P_{eff,\ passive}$ for an intestinal segment (duodenum, jejunum, ileum and colon) is a function of P_{trans}, P_{para}, intestinal segment scaling factor (k_{GI}) and unstirred boundary layer (UBL) permeability (P_{UBL}) as described by the following **Equation**[4,5]**:**

$$P_{eff,passive} = (P_{trans} + P_{para}) \times k_{GI} \times \frac{P_{UBL}}{(P_{trans}+P_{para})+P_{UBL}}$$

Table 1. *The applied parameters used in the MPP-model. Compound and system parameters are presented in green and red, respectively.*

Parameter	Abbreviation	Number	Unit
Accessibility surface scalar	Acc	1	-
(Spherical) molecular radius	r	3.6	Å
Diffusion coefficient	D	9.39x 10^{-6}	cm^2/s
fraction of neutral species	f_0	~0	-
fraction of negatively charged species	f_z	1	-
Octanol-water partition coefficient	$P_{o:w}$	2.69x10^{-4}	-
Porosity/Pore-length	ε/δ	0.466	cm^{-1}
UBL height	h_{UBL}	30	µm
Paracellular pore radius in segment	R		Å
• Duodenum		8.8	
• Ileum		3.8	
• Colon		2.3	
Villi Expansion	VE		-
• Duodenum/jejunum		10	
• Ileum		10	
• Colon		1	
Fold expansion	FE		-
• Duodenum/jejunum		3	
• Ileum		3	
• Colon		1	

$$P_{para} = \frac{\varepsilon}{\delta} \times D \times F\left(\frac{r}{R}\right) \times (f_0 + f_z \times 0.24)$$

$$P_{trans} = 2.36 \times 10^{-6} \times {P_{o:w}}^{1.1}$$

$$k_{GI} = VE \times FE \times Acc$$

$$P_{UBL} = D / h_{UBL}$$

Scheme 1. *The applied parameters in MPP-model. Compound and system parameters presented in green and red, respectively.*

Presented at the 19th North American ISSX / 29th JSSX Meeting in San Francisco, CA, USA October 19-23, 2014

Methods, continued

PBPK models

The population based Simcyp Simulator (V12-R2) was used to build four PBPK models for acamprosate,

Model 1: PBPK-iv,$CL_{R,GF}$
Model 2: PBPK-iv,$CL_{R,GF}$ + $CL_{R,car}$
Model 3: PBPK-$_{oral,}$ $P_{eff,passive}$
Model 4: PBPK-$_{oral,}$ $P_{eff,passive}$ + $CL_{R,car}$

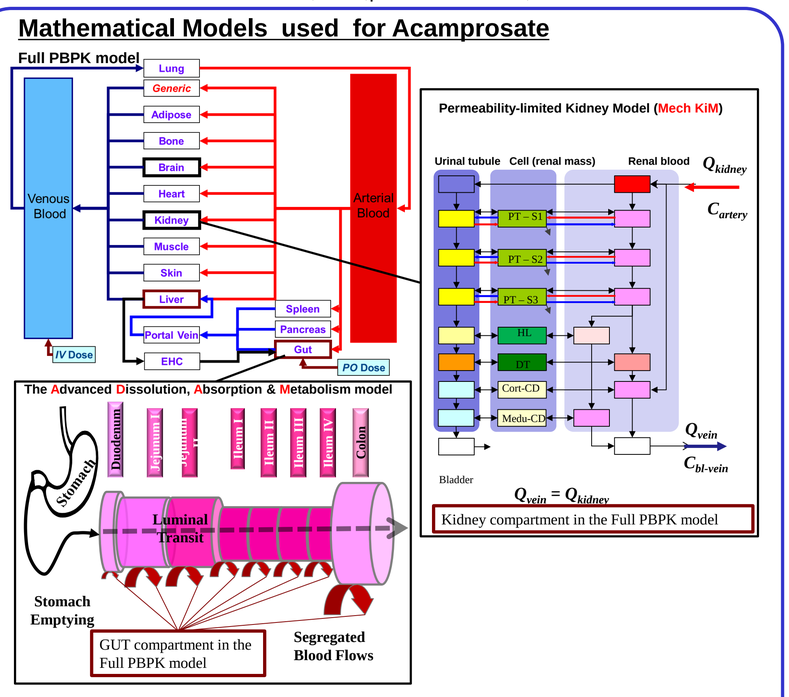

Figure 2. *For Model 1 and 2 two submodels were used, i.e. the Simcyp full-PBPK distribution model (Rodgers and co-workers) and the permeability-limited mechanistic kidney model (Mech KiM). For Model 3 and 4 a permeability-limited model for the gut, i.e. the advanced dissolution absorption and metabolism (ADAM) was additionally applied.*

In vitro inhibition studies

Acamprosate inhibition of probe influx or efflux, by nine selected transporters, was investigated *in vitro* using Caco-2 cells from "Deutsche Sammlung von Mikroorganismen und Zellkulturen" (DSMZ) (Table 2). Passage numbers 2-11 were used and influx or efflux were conducted as described previously[6] on day 11 or 21 after seeding 8.93•10^{-4} cells/cm^2 on bottom of wells or on filters, respectively.

Table 2. *The probes/tritrium labelled compounds applied to screen for acamprosate interaction on selected transporters*

Probe	Carrier gene	Carrier protein
[^{14}C]-Gly-Sar	SLC15A *SLC36A1*	Peptide tansporter 1 (PEPT1) H^+/Amino acid transporter 1 (PAT1)
[^{3}H]-taurine	SLC6A6 *SLC36A1*	Taurine transporter (TAUT) H^+/Amino acid transporter 1 (PAT1)
[^{3}H]-glutamat	*SLCA3/1*	Excitatory amino-acid transporters (EAAT1/3)
[^{3}H]-proline	*SLC36A1*	H^+/Amino acid transporter 1 (PAT1)
[^{3}H]-lysine	*SLC7A9/SLC3A1*	Glycoprotein-associated amino acid transporter/Neutral and basic amino acid transport protein ($B^{0,+}$AT/rBAT)
[^{3}H]-Estrone-3-sulfate	*SLCO2B1* SLC51A/B	Organic anion transporter polypeptide 2B1 (OATP2B1) Organic solute transporter α/β (OST-α/β)
[^{3}H]-taurocholic acid	*SLC10A2*	Apical sodium dependent bile acid transporter (ASBT)

Results

P_{para} determines $P_{eff,\ passive}$

- P_{UBL} was calculated to 31.3•10^{-4} cm/s, and does not limit P_{para} and P_{trans}.
- It is mainly P_{para} that contributes to overall acamprosate $P_{eff,\ passive}$ (Table 3)
- P_{para} is to a large extent influenced by the molecular- to pore-radius ratio (r/R) (Table 3, Figure 3).

Table 3. *Estimates of $P_{eff,passive}$ used in PBPK-$_{oral,}$ $P_{eff,passive}$ and the final PBPK-$_{oral,}$ $P_{eff,passive}$ +P_{car}*

Intestinal segment	r/R	P_{para} (10^{-6} cm/s)	P_{trans} (10^{-6} cm/s)	k_{GI}	$P_{eff,\ passive}$ (10^{-4} cm/s)	fa
Duodenum/ Jejunum	0.41	0.0979	0.0003	30	0.0293	0.0055
Ileum	0.95	0.0001	0.0003	10	<0.0001	<0.0001
Colon	<1	0	0.0003	1	<0.0001	<0.0001

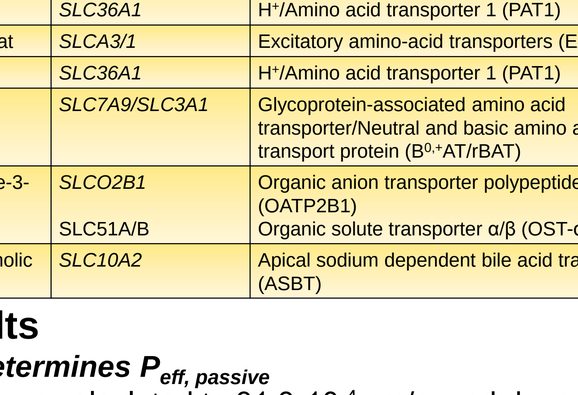

Figure 3. *Relation between paracellular permeability (P_{para}) and the molecular- to-pore radius ratio (r/R). The molecular radius for acamprosate was calculated as 3.6 Å.*

Results, continued

P_{para} underestimates acamprosate oral exposure

The simulation of disposition and clearance of acamprosate is, for our purpose, acceptably predicted (Figure 4, top). Hence, it is the estimation of acamprosate oral absorption -and not disposition or clearance- that mainly discriminates between the simulated and observed plasma-concentration-time profiles after oral administration of acamprosate.

The simulated area under the curve (AUC) of the acamprosate plasma concentration-time profile after oral administration, using segmental $P_{eff,\ passive}$ input (which almost exclusively is determined by P_{para} ,Table 3), is underpredicted (Figure 4, bottom). When the fitted net absorptive P_{car} is added to $P_{eff,\ passive}$, the prediction of acamprosates plasma concentration-time profile is improved.

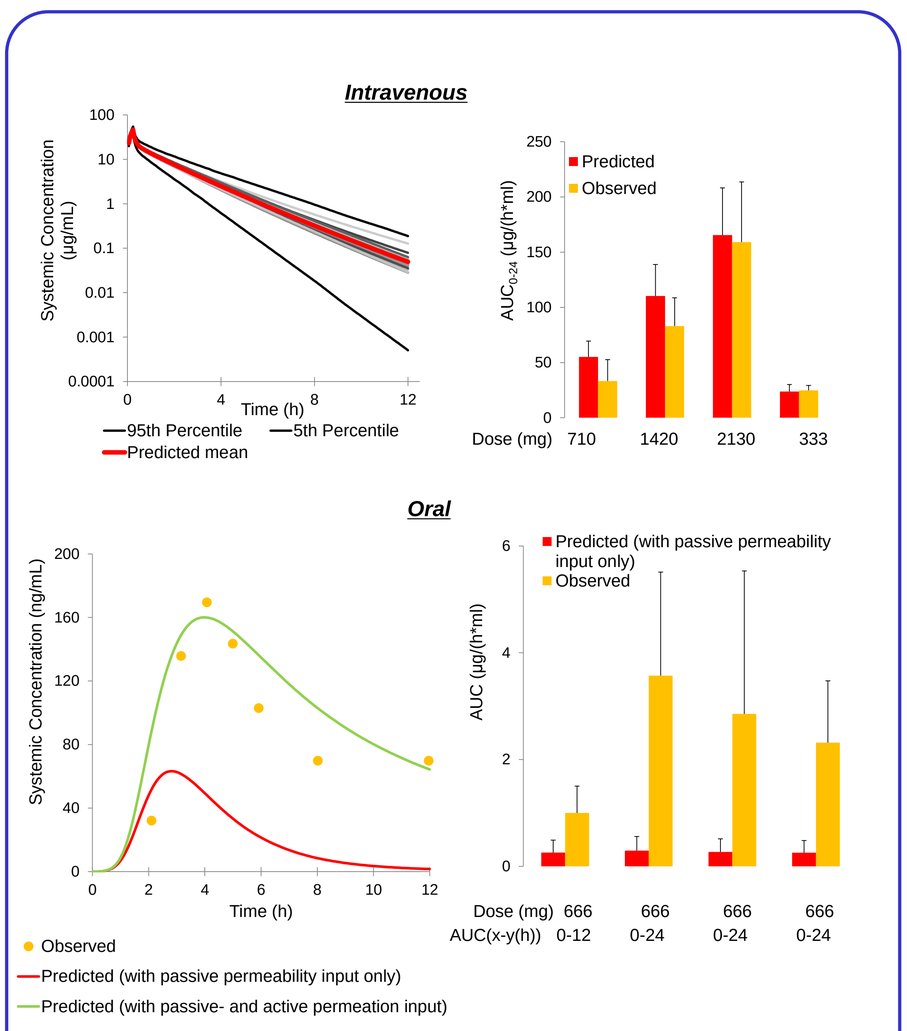

Figure 4. *Acamprosate PBPK model simulation of plasma concentration-time profiles and AUC compared to clinical studies. All studies are single-dose studies. The concentration-time profiles are given after a 666 mg dose.*

Acamprosate inhibits carrier-mediated taurine and glutamate uptake

Acamprosate inhibited [^{3}H]-taurine uptake via TAUT and [^{3}H]-glutamate uptake via EAAT1/3, which resulted in the IC_{50} values of 69.1 and 183.3 mM, respectively.

Conclusions

- Acamprosate intestinal absorption in human seems to be partly paracellular and partly mediated by yet unidentified membrane transporters.
- Acamprosate intestinal absorption in human is negligibly influenced by passive diffusion-driven transcellular- and unstirred boundary layer permeability.
- Acamprosate inhibits TAUT-mediated taurine influx in mM concentrations. Further *in vitro* transporter studies are required to identify which other transporters may be involved in acamprosate absorption. Corresponding *in vivo* intestinal transporter abundance and activity data are then desirable to allow *in vitro-in vivo* extrapolation for these transporters.
- *In vitro* transport studies in combination with modelling and simulation is a powerful combination of tools to investigate mechanisms of intestinal absorption.

Acknowledgements

We would like to thank Per Holm (PhD) and Frank Larsen (PhD), chief specialists at Lundbeck A/S for their help in offering us the resources in running this study. We would like to acknowledge Lundbeck A/S and the Drug Research Academy, University of Copenhagen, for co-financing this project.

References

1. Chabenat C, Chretien P, Daoust M, Moore N, Andre D, Lhuintre JP, Salogaut C, Biosmare F (1988) Physicochemical, pharmacological and pharmacokinetic study of a new GABAergic compound calcium acetylhomotaurine, Methods Find Exp Clin Pharmacol 10, 311-317.
2. Saivin S, Hulot T, Chabac S, Potgieter A, Durbin P, Houlin G (1998) Clinical pharmacokinetics of acamprosate, Clin Pharmacokinet 35, 331-345.
3. Zornosa T, Cano-Cebrián MJ, Nalda-Molina R, Guerri C, Granero L, Polache A (2004) Assessment and modulation of acamprosate intestinal absorption: comparative studies using in situ, in vitro (Caco-2 cell monolayers) and in vivo models, Eur J Pharm Sci 22, 347-356.
4. Sugano, K. (2009) Theoretical investigation of passive intestinal membrane permeability using Monte Carlo method to generate drug-like molecule population. Int J Pharmaceutics 373(1), 55-61.
5. Adson, A., Raub, T. J., Burton, P. S., Barsuhn, C. L., Hilgers, A. R., Ho, N. F., & Audus, K. L. (1994) Quantitative approaches to delineate paracellular diffusion in cultured epithelial cell monolayers. J Pharm Sci 83(11), 1529-1536.
6. Grandvuinet AS, Gustavsson L, Steffansen B (2013) New insights into the carrier mediated transport of estrone-3-sulfate in the Caco-2 cell model Mol Pharm 10, 3285-3295.